THE ASTROPHYSICAL JOURNAL, 316:788–800, 1987 May 15

THE INFLUENCE OF THE CORIOLIS FORCE ON FLUX TUBES RISING THROUGH THE SOLAR CONVECTION ZONE

ARNAB RAI CHOUDHURI AND PETER A. GILMAN
High Altitude Observatory, National Center for Atmospheric Research[1]
Received 1986 September 19; accepted 1986 November 4

ABSTRACT

One hypothesis currently under active study is that solar magnetic fields are generated by dynamo action at the bottom of the convection zone, and then rise through the zone to the photosphere due to magnetic buoyancy. In order to study the effect of the Coriolis force due to solar rotation on the rising magnetic flux, we consider a flux ring, azimuthally symmetric around the rotation axis, starting from rest at the bottom of the convection zone, and then we follow the trajectory of the flux ring as it rises. If we assume the flux ring remains azimuthally symmetric during its ascent, then the problem can be described essentially in terms of two parameters: the value of the initial magnetic field in the ring when it starts, and the effective drag experienced by it (which is related to the radius of cross section of the ring). For field strengths at the bottom of the convection zone of order 10^5 G or less, we find that the Coriolis force plays a dominant role and flux rings starting from low latitudes at the bottom are deflected and emerge at latitudes significantly poleward of sunspot zones. We discuss implications of this result for the Sun and for other stars.

Subject headings: convection — hydromagnetics — Sun: interior — Sun: magnetic fields

I. INTRODUCTION

During the last few years, the bottom of the solar convection zone is increasingly drawing the attention of solar physicists as the likely site for the operation of the solar dynamo. The overshoot region underneath the convection zone has been estimated to have a thickness of a fraction of scale height (van Ballegooijen 1982; Schmitt, Rosner, and Bohn 1984). A dynamo operating in this region may circumvent some of the difficulties besetting those models which assumed dynamo action to take place in the convection zone. One of the major difficulties with convection zone dynamos is that magnetic buoyancy would rather quickly remove any magnetic flux from the convection zone without allowing sufficient time for dynamo amplification (Parker 1975; Moreno-Insertis 1983). The overshoot region is believed to be a better place for the storage and amplification of magnetic flux (Parker 1975; Spiegel and Weiss 1980; Galloway and Weiss 1981; Spruit and van Ballegooijen 1982; van Ballegooijen 1982). Probably this stored flux ultimately gets broken loose by the doubly diffusive instabilities and rises through the convection zone (Schmitt and Rosner 1982). Another difficulty with the convection zone dynamo is that, though the kinematical models of the solar dynamo were remarkably successful in reproducing the butterfly diagram and other observed features (see Moffatt 1978, pp. 234–243, for a review), more recent self-consistent dynamical calculations suggest that those kinematical models are not internally consistent (Gilman and Miller 1981; Gilman 1983; Glatzmaier 1985). In the kinematical models, the differential rotation and the cyclonic convection are independently adjusted to reproduce the butterfly diagrams. However, when one tries to obtain both differential rotation and convection together from a self-consistent scheme, one finds that the values used in kinematical models for the best fit are mutually incompatible. Though the current dynamical models predict a poleward drift of dynamo waves, in contradiction with observations, it may be possible to get an equatorward drift by restricting the dynamo to the bottom of the convection zone (Glatzmaier 1985). Only recently the properties of a dynamo in the overshoot region have begun to be studied in a quantitative fashion (DeLuca and Gilman 1986). If solar magnetic fields are produced in the overshoot region, then the convection zone can be thought of as a region through which the fields rise to the photosphere because of magnetic buoyancy or other effects.

The idea of magnetic buoyancy was first suggested by Parker (1955), and it has since been studied through two different approaches. One approach is to consider a continuous distribution of magnetic field and study its stability (Gilman 1970; Acheson 1978). The other approach is to study the behavior of a flux tube embedded in a nonmagnetic atmosphere (Spruit and van Ballegooijen 1982). Here we shall follow the flux tube approach. If magnetic fields are broken loose from the overshoot region due to double diffusive instabilities (Schmitt and Rosner 1982), then indeed we expect them to rise through the convection zone in the form of flux tubes. The aim of the present paper is to understand the effect of solar rotation on these rising flux tubes. The effect of rotation on magnetic buoyancy instability for a continuous field distribution has already been studied (Gilman 1970; Roberts and Stewartson 1977; Acheson and Gibbons 1978; Acheson 1978, 1979; Schmitt and Rosner 1982; Hughes 1985), and it is seen that rotation can slow down the rate of instability growth. The analogous problem for flux tubes was treated by van Ballegooijen (1983). However, we believe that we are the first to consider how rotation can deflect the trajectories of flux tubes rising through the solar convection zone. Especially, our aim has been to determine whether flux tubes starting from low latitudes at the bottom of the convection zone can be deflected enough by the Coriolis force to emerge eventually at a much higher latitude on the solar surface. As a result of our calculations, we have come to the conclusion that the Coriolis force plays a much more important role in this problem than has been recognized so far.

[1] The National Center for Atmospheric Research is sponsored by the National Science Foundation.

The magnitude of the magnetic buoyancy effect is determined by the magnetic field strength, which dictates the density decrease inside the tube compared to its surroundings at a given ambient pressure level. A plausible estimate of this density difference $\Delta\rho$ can be made by considering a tube in total pressure and temperature equilibrium with its surroundings (in the detailed calculations below, we consider more general thermal conditions). Then

$$\Delta\rho/\rho_e = B^2/8\pi p_e \tag{1}$$

in which ρ_e, p_e are the density and gas pressure external to the tube.

If the magnetic field at these levels is maintained by a dynamo, and the magnetic fields are diffuse, then the field strength is unlikely to be more than $\sim 10^4$ G, because larger fields would severely inhibit dynamo action (DeLuca and Gilman 1986). The fields are also unlikely to be much less in amplitude, if they are responsible for the flux seen in emerging active regions at the solar surface (Galloway and Weiss 1981). If there is a mechanism to concentrate the fields into individual isolated flux tubes, such as obviously occurs near the top of the solar convection zone, then field strengths an order of magnitude larger are possible. From equation (1), with $p_e \approx 5 \times 10^{13}$ dyn cm^{-2} at the bottom of the convection zone, $\Delta\rho/\rho = 10^{-5}$ occurs for $B \approx 1.1 \times 10^5$ G, $\Delta\rho/\rho = 10^{-7}$ for 1.1×10^4 G.

In the absence of Coriolis forces, a flux ring rising due to magnetic buoyancy but unaffected by drag would achieve a velocity $v \approx [2(\Delta\rho/\rho)gl]^{1/2}$ by accelerating through a length l. Then for gravity $g \approx 5 \times 10^4$ cm^2 s^{-1}, and $l = 3 \times 10^9$ cm, we get $v \approx 0.58$ km s^{-1} for $B = 1.1 \times 10^5$ G, and 0.058 km s^{-1} for $B = 1.1 \times 10^4$ G. The ratio of Coriolis force to magnetic buoyancy force, $|2\Omega \times v|/|(\Delta\rho/\rho)g| \approx 0.58$ for $B = 1.1 \times 10^5$ G and ~ 5.8 for $B = 1.1 \times 10^4$ G. Consequently, we should expect Coriolis forces to be important for flux tubes rising from the bottom of the convection zone for a wide range of magnetic field strengths.

Once a flux tube is loosened from the overshoot region, it rises due to magnetic buoyancy. For the sake of simplicity, we restrict our first calculations presented here only to the axisymmetric case. In our model, a circular ring of flux starts from the bottom of the convection zone and rises while maintaining its symmetric shape. However, it is interesting to note that Schüssler (1980) has argued that such a flux ring will tend to maintain its symmetric shape during most of its rise through the convection zone and may become unstable to loop formations only in the very top layers. After presenting the results of our calculations, in § V we discuss the implications of our results for Schüssler's arguments and also consider what kind of changes we may expect in our final results if we were to relax the simplifying assumption of axisymmetry. It has been suggested that the top of the convection zone may be like an impervious boundary and may influence the motion of flux tubes in the underlying layers (Parker 1984; Choudhuri 1984). However, in the present calculations, we allow the flux rings to move freely to the top of the convection zone. Recently Parker (1986) pointed out the possibility that thermal shadows may play some role in suppressing magnetic buoyancy. Quantitative tests of this concept have yet to be worked out so we neglect thermal shadows in the present paper.

In the next section we derive and discuss the equations governing the motion of axisymmetric flux rings. Two of the most uncertain aspects of the problem are the treatment of drag and the treatment of heat exchange between the flux tube and its surroundings. In § III we neglect the drag and present the results of calculations done with the two extreme assumptions of the flux ring being always in thermal equilibrium with its surroundings, and the flux ring being completely adiabatic. The results turn out to be qualitatively alike. A discussion of drag is presented in § IV, where we show how our results of § III are modified. Finally the conclusions are summarized in the last section.

II. FORMULATION OF THE PROBLEM

a) *The Equation of Motion for a Flux Ring*

We consider a flux ring, azimuthally symmetric around the axis of rotation, embedded in the convection zone. Let the radius of cross section σ of the tube be small compared to solar radius ($\sigma \ll R_\odot$) so that the position of the ring can be described by a pair of coordinates (r, θ). In order to study the effect of rotation on this flux ring, we neglect the variation of angular velocity over the convection zone, assuming it to rotate as a solid body. The effect of differential rotation is discussed in § V and Appendix B. Let $\boldsymbol{\Omega}$ be the angular velocity of the convection zone and let $\boldsymbol{v}$ be the fluid velocity with respect to a frame of reference corotating with angular velocity $\boldsymbol{\Omega}$. The equation of motion for a fluid element inside or around the flux ring is

$$\rho\left(\frac{D\boldsymbol{v}}{Dt} + 2\boldsymbol{\Omega} \times \boldsymbol{v}\right) = -\nabla(p_e + p_1) + \frac{(\nabla \times \boldsymbol{B}) \times \boldsymbol{B}}{4\pi} + \rho\boldsymbol{g}' + \boldsymbol{F}_{\text{drag}}, \tag{2}$$

where $\boldsymbol{g}' = \boldsymbol{g} - \nabla(|\boldsymbol{\Omega} \times \boldsymbol{r}|^2)$ includes the centrifugal force, and p_e is the value the pressure would have in the absence of the flux ring, whereas the part p_1 is due to the presence of the flux ring (see, for example, Acheson and Hide 1973). In the solar convection zone, the centrifugal force is negligible compared to gravity so that we shall be using $\boldsymbol{g}' = \boldsymbol{g}$ for our calculations.

We now make the simplifying assumption that variations of different physical quantities within the flux ring are small. This assumption holds if the radius σ of the flux ring is small compared to the pressure scale height Λ (see Schüssler 1979 for a discussion about this assumption). Using subscripts i and e to denote physical quantities inside and outside the flux ring, and remembering that $\nabla p_e = \rho_e \boldsymbol{g}$, we integrate equation (2) over the flux ring. This yields

$$m_i\left(\frac{D\boldsymbol{u}}{Dt} + 2\boldsymbol{\Omega} \times \boldsymbol{u}\right) = (m_i - m_e)\boldsymbol{g} + \int dv \frac{(\nabla \times \boldsymbol{B}) \times \boldsymbol{B}}{4\pi} + \int dv(\boldsymbol{F}_{\text{drag}} - \nabla p_1),$$

where $m_i = \rho_i \pi\sigma^2 \cdot 2\pi r \sin\theta$, $m_e = \rho_e \pi\sigma^2 \cdot 2\pi r \sin\theta$, and $\boldsymbol{u}$ is the velocity of the flux ring. The net drag on the flux ring, $\int dv(\boldsymbol{F}_{\text{drag}} - \nabla p_1)$, has both a dissipative part and a nondissipative part. The nondissipative part arises due to the fact that the motion of the flux ring imparts kinetic energy to the surrounding fluid and can be taken account of by replacing m_i by $m_i + m_e \approx 2m_i$ in that component of the acceleration term which is perpendicular to the ring[2] (Lamb 1945, p. 77). Writing

[2] This is actually a result for incompressible fluids. However, since we shall be dealing mostly with highly subsonic motions in this paper, replacing m_i by $2m_i$ should be a fairly good approximation for our purposes.

the dissipative part of the drag as $\boldsymbol{D}$, we have

$$2m_i\left(\frac{D\boldsymbol{u}}{Dt}+2\boldsymbol{\Omega}\times\boldsymbol{u}\right)_{\perp}+m_i\left(\frac{D\boldsymbol{u}}{Dt}+2\boldsymbol{\Omega}\times\boldsymbol{u}\right)\cdot\hat{\boldsymbol{e}}_\phi\hat{\boldsymbol{e}}_\phi$$
$$=(m_i-m_e)\boldsymbol{g}+\int dv\,\frac{(\nabla\times\boldsymbol{B})\times\boldsymbol{B}}{4\pi}+\boldsymbol{D}\,. \quad (3)$$

For a magnetic field $\boldsymbol{B}=B\hat{\boldsymbol{e}}_\phi$ inside the flux ring (B being constant) and zero elsewhere, the tension term can be shown to be

$$\int dv\,\frac{(\nabla\times\boldsymbol{B})\times\boldsymbol{B}}{4\pi}=-\frac{\pi\sigma^2\sin\theta}{2}(B^2\cot\theta\hat{\boldsymbol{e}}_\theta+B^2\hat{\boldsymbol{e}}_r)$$
$$=-\frac{\Psi^2}{2\pi\sigma^2}(\cos\theta\hat{\boldsymbol{e}}_\theta+\sin\theta\hat{\boldsymbol{e}}_r)\,,$$

where $\Psi=\pi\sigma^2B$ is the transverse flux through the ring. Using the expression of acceleration in spherical coordinates (see, for example, Symon 1971), we can write down the three components of equation (3):

$$2m_i\left[\frac{d^2r}{dt^2}-r\left(\frac{d\theta}{dt}\right)^2-r\left(\frac{d\phi}{dt}\right)^2\sin^2\theta-2r\Omega\left(\frac{d\phi}{dt}\right)\sin^2\theta\right]$$
$$=-(m_i-m_e)g_s\left(\frac{R_\odot}{r}\right)^2-\frac{\Psi^2}{2\pi\sigma^2}\sin\theta+D_r\,, \quad (4)$$

$$2m_i\left[r\frac{d^2\theta}{dt^2}+2\frac{dr}{dt}\frac{d\theta}{dt}-r\left(\frac{d\phi}{dt}\right)^2\sin\theta\cos\theta\right.$$
$$\left.-2r\Omega\left(\frac{d\phi}{dt}\right)\sin\theta\cos\theta\right]=-\frac{\Psi^2}{2\pi\rho^2}\cos\theta+D_\theta\,, \quad (5)$$

and

$$m_i\left[r\frac{d^2\phi}{dt^2}\sin\theta+2\frac{dr}{dt}\frac{d\phi}{dt}\sin\theta+2r\frac{d\theta}{dt}\frac{d\phi}{dt}\cos\theta\right.$$
$$\left.+2\Omega\left(r\frac{d\theta}{dt}\cos\theta+\frac{dr}{dt}\sin\theta\right)\right]=D_\phi\,. \quad (6)$$

Here, g_s in equation (4) is the surface gravity. Neglecting the self-gravity of the convection zone (which contains less than 2% of solar mass), we have written $\boldsymbol{g}=-g_s(R_\odot/r)^2\hat{\boldsymbol{e}}_r$.

Let us now transform to the dimensionless coordinates $\xi=r/R_\odot$ and $\tau=10^{-3}t(g_s/R_\odot)^{1/2}$. Then equations (4)–(6) become

$$\ddot{\xi}-\xi\dot{\theta}^2-\xi\dot{\phi}^2\sin^2\theta-2\omega\xi\dot{\phi}\sin^2\theta$$
$$=\frac{M(\xi,\theta)}{\xi^2}-\frac{T}{A(\xi,\theta)}\sin\theta+D_r'(\xi,\theta,\boldsymbol{u})\,, \quad (7)$$

$$\xi\ddot{\theta}+2\dot{\xi}\dot{\theta}-\xi\dot{\phi}^2\sin\theta\cos\theta-2\omega\xi\dot{\phi}\sin\theta\cos\theta$$
$$=-\frac{T}{A(\xi,\theta)}\cos\theta+D_\theta'(\xi,\theta,\boldsymbol{u})\,, \quad (8)$$

$$\xi\ddot{\phi}\sin\theta+2\dot{\xi}\dot{\phi}\sin\theta+2\xi\dot{\theta}\dot{\phi}\cos\theta+2\omega(\xi\dot{\theta}\cos\theta+\dot{\xi}\sin\theta)$$
$$=D_\phi'(\xi,\theta,\boldsymbol{u})\,, \quad (9)$$

where $\omega=10^3\Omega/(g_s/R_\odot)^{1/2}$ is the dimensionless rotation parameter, $M(\xi,\theta)=10^6\times(\rho_e-\rho_i)/2\rho_i$ is the dilution factor and is a measure of magnetic buoyancy, $A(\xi,\theta)=\sigma^2(\xi,\theta)/\sigma^2(\xi_0,\theta_0)$ is the ratio of ring cross sectional area to the area at the bottom, $\xi=\xi_0$, of the convection zone, $T=10^6\Psi^2/4\pi m_i g_s\sigma^2(\xi_0,\theta_0)=10^6B_0{}^2/8\pi\rho_i(\xi_0)g_s\xi_0R_\odot\sin\theta_0$ is a dimensionless measure of the magnetic tension, and $\boldsymbol{D}'(\xi,\theta,\boldsymbol{u})=(10^6/2m_ig_s)(D_r\hat{\boldsymbol{e}}_r+D_\theta\hat{\boldsymbol{e}}_\theta+2D_\phi\hat{\boldsymbol{e}}_\phi)$ is the drag. All dots denote differentiation with respect to τ. In equations (7)–(9) we have indicated explicitly which quantities depend on ξ and θ in a spherically stratified convection zone. For the solar values $g_s=2.74\times10^4$ cm s^{-2}, $R_\odot=6.96\times10^{10}$ cm, $\Omega=2.8\times10^{-6}$ s^{-1}, we have $\omega=4.4$, $\tau=6.3\times10^{-7}t$ (t in seconds) and $\dot{\xi}=2.3dr/dt$ (dr/dt in km s^{-1}). Thus $\tau=1$ corresponds to 18 days, and $\dot{\xi}=1$ corresponds to a speed of 0.43 km s^{-1}. The dimensionless variables are introduced in such a way that all the terms in the equations of motion become roughly of order unity for our problem.

We see from equations (7)–(9) that the motion of the flux ring is essentially driven by four forces:

(1) Magnetic buoyancy [represented by $M(\xi,\theta)$].
(2) Coriolis force (represented by terms involving ω).
(3) Magnetic tension [represented by $T/A(\xi,\theta)$].
(4) Drag (represented by $\boldsymbol{D}'$).

It has already been noted that the Coriolis force is comparable with buoyancy when the magnetic field is 10^5 G or less, i.e., $M(\xi,\theta)<5$. Let us now consider the strength of magnetic tension relative to magnetic buoyancy. For a flux tube in thermal equilibrium with surroundings,

$$\frac{T/A(\xi,\theta)}{M(\xi,\theta)}=\left(\frac{\rho_ig_sr\sin\theta}{2p_i}\right)^{-1}.$$

Using $p=5\times10^{13}$ dyn cm^{-2}, $\rho=0.2$ g cm^{-3} for the bottom of the convection zone (taken at $\xi=0.7$), and $p=1.5\times10^5$ dyn cm^{-2}, $\rho=3\times10^{-7}$ g cm^{-3} for the top, the above ratio turns out to be 0.24 cosec θ and 5×10^{-3} cosec θ, respectively, for the bottom and the top. Hence, the magnetic tension may have some importance when the flux rings start, but it becomes negligible as the rings reach the upper surface. If the flux tube is adiabatic, then magnetic tension becomes unimportant even more quickly.

b) *Flux Ring in the Convection Zone*

To proceed further, we have to understand how to estimate the area increment factor $A(\xi,\theta)$ and the magnetic buoyancy factor $M(\xi,\theta)$. For this we need a model of the background convection zone, which we assume to be adiabatically stratified with a small superadiabatic gradient. This superadiabatic gradient can have considerable effect on the magnetic buoyancy of a flux tube displaced adiabatically, but we can neglect it while calculating a model of the convection zone. Using the perfect gas law $p_e=R\rho_eT_e$, with constant ratio of specific heats γ, it follows that

$$T_e=T_{e,0}-\beta\left(\frac{\xi-\xi_0}{\xi}\right),\quad(\xi_0<\xi<1) \quad (10)$$

where

$$\beta=\left(\frac{\gamma-1}{\gamma}\right)\frac{g_sR_\odot}{R}\,, \quad (11)$$

and $T_{e,0}$ is the temperature at the bottom. If $p_{e,0}$ be the pressure and density at the bottom,

$$p_e=p_{e,0}\left(\frac{T_e}{T_{e,0}}\right)^{\gamma/(\gamma-1)},\quad \rho_e=\rho_{e,0}\left(\frac{T_e}{T_{e,0}}\right)^{1/(\gamma-1)}. \quad (12)$$

Let our flux ring start with the same temperature $T_{i,0} = T_{e,0} = T_0$ as the surroundings at the bottom (the pressure and density being $p_{i,0}$ and $\rho_{i,0}$). The area increment factor $A(\xi, \theta)$ is always given by (neglecting the higher order terms arising from the small difference between ρ_i and ρ_e)

$$A(\xi, \theta) = \frac{\rho_{i,0}\,\xi_0 \sin\theta_0}{\rho_i\,\xi \sin\theta} = \left[1 - \frac{\beta(\xi - \xi_0)}{T_0\,\xi}\right]^{-1/(\gamma-1)} \left(\frac{\xi_0 \sin\theta_0}{\xi \sin\theta}\right). \quad (13)$$

If we assume the flux ring to be always in thermal equilibrium with the surroundings, then the magnetic buoyancy factor $M(\xi, \theta) = \frac{1}{2} \times 10^6(\Delta\rho/\rho)$ is given by

$$M(\xi, \theta) = \frac{10^6 B^2}{16\pi p_e} = \frac{10^6 B_0^{\,2}}{16\pi p_{e,0}} \left(\frac{T_i}{T_0}\right)^{(2-\gamma)/(\gamma-1)} \left(\frac{\xi \sin\theta}{\xi_0 \sin\theta_0}\right)^2 = M(\xi_0, \theta_0)\left[1 - \frac{\beta(\xi - \xi_0)}{T_0\,\xi}\right]^{(2-\gamma)/(\gamma-1)} \left(\frac{\xi \sin\theta}{\xi_0 \sin\theta_0}\right)^2. \quad (14)$$

On the other hand, if the flux ring moves adiabatically, keeping only the lowest order terms, we find

$$\frac{\Delta\rho}{\rho} \approx \frac{B_0^{\,2}}{8\pi p_{e,0}}\left[\frac{1}{\gamma}\left(\frac{T_e}{T_0}\right)^{(2-\gamma)/(\gamma-1)} \left(\frac{\xi \sin\theta}{\xi_0 \sin\theta_0}\right)^2 + \left(1 - \frac{1}{\gamma}\right)\right] + \frac{\Delta S(\xi)}{C_p}, \quad (15)$$

where $\Delta S(\xi)$ is the difference in entropy per unit mass between the inside and the outside of the flux ring (see Moreno-Insertis 1983 for details) and C_p is the specific heat at constant pressure. It is easy to show that

$$\frac{\Delta S(\xi)}{C_p} = \int_{\xi_0}^{\xi} \frac{\nabla\Delta T}{T_e} R_\odot\, d\xi, \quad (16)$$

where $\nabla\Delta T = (dT/dr) - (dT/dr)_{\rm ad}$ is the superadiabatic gradient. According to mixing length theory, the solar luminosity is given by

$$L_\odot = 4\pi r^2 \rho_e C_p \kappa \nabla\Delta T, \quad (17)$$

where κ is the diffusion coefficient for the eddies. Substituting from equation (17) in equation (16) we get

$$\frac{\Delta S(\xi)}{C_p} = \frac{(\gamma - 1)L_\odot}{4\pi\gamma R_\odot} \int_{\xi_0}^{\xi} \frac{d\xi'}{\kappa \xi'^2 p_{e,0}\{1 - [\beta(\xi' - \xi_0)/T_0\,\xi']\}^{\gamma/(\gamma-1)}}. \quad (18)$$

Thus, for adiabatic flux rings in a superadiabatic convection zone, we have from equation (15)

$$M(\xi, \theta) = M(\xi_0, \theta_0)\left[\frac{1}{\gamma}\left(\frac{T_e}{T_0}\right)^{(2-\gamma)/(\gamma-1)} \left(\frac{\xi \sin\theta}{\xi_0 \sin\theta_0}\right) + \left(1 - \frac{1}{\gamma}\right)\right] + \frac{10^6 \Delta S(\xi)}{2C_p} \quad (19)$$

with the last term given by equation (18).

III. RESULTS WITHOUT DRAG

We found that the standard models of the convection zone (Spruit 1974; Däppen and Gough 1984) are approximated fairly well by the following choices of the parameters:

$$T_0 = 2.2 \times 10^6 \text{ K},$$
$$p_{e,0} = 5.8 \times 10^{13} \text{ dyn cm}^{-2},$$
$$\beta = 7313 \times 10^3 \text{ K},$$

and

$$\gamma = 1.41.$$

(See eqs. [10] and [12]. We have taken $\xi_0 = 0.7$.) We now solve equations (7)–(9) as an initial value problem with a flux ring starting from rest (i.e., $\dot\xi = \dot\theta = \dot\phi = 0$) at the bottom of the convection zone ($\xi_0 = 0.7$, θ_0, $\phi_0 = 0$). We use the solar value $\omega = 4.4$, and for our choice of parameters, $T = 0.25M(\xi_0, \theta_0)$ cosec θ_0. We evaluate $A(\xi, \theta)$ from equation (13) and put $\boldsymbol{D}'(\xi, \theta, \boldsymbol{u}) = 0$. Calculations are made for the following three cases:

1. The flux rings are assumed to be always in thermal equilibrium with the surroundings so that the magnetic buoyancy factor $M(\xi, \theta)$ is given by equation (14).
2. The rings are assumed to rise adiabatically in a convection zone without a superadiabatic gradient so that $M(\xi, \theta)$ is given by equation (19) without the last term.
3. Adiabatic rings are in a superadiabatic convection zone so that $M(\xi, \theta)$ is given by equation (19) with the superadiabatic term estimated from equation (18).

The motivation behind considering cases (2) and (3) separately is to isolate the effect of the superadiabatic gradient in this problem. We take $\kappa = 10^{13}$ cm^2 s^{-1} to estimate the superadiabatic term. This term, $10^6\Delta S(\xi)/2C_p$, is plotted in Figure 1. It is easy to see that this term is very small at the bottom of the convection zone. However, near the upper surface, it eventually becomes the dominant term and tends to be quite large compared to other terms in equation (19). The total variation is about five orders of magnitude.

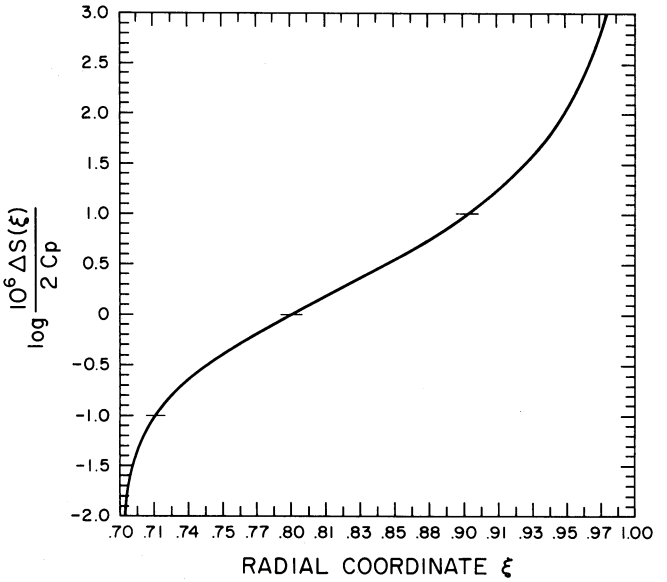

FIG. 1.—The superadiabatic term $10^6\Delta S(\xi)/2C_p$ appearing in eq. (19) as a function of depth of the convection zone. The marks on the curve correspond to places where the superadiabatic term equals the initial magnetic buoyancy $M(\xi_0, \theta_0) = 1/10, 1, 10$.

We used the HAO VAX 11-750 to integrate our equations with the help of the program ODEN for solving initial value problems. For each of the three cases we solved the problem with three values of the magnetic buoyancy factor $M(\xi_0, \theta_0) = 10, 1, 1/10$, which correspond to $(\Delta\rho/\rho)_0 = 2 \times 10^5, 2 \times 10^{-6}, 2 \times 10^{-7}$, or equivalently to initial fields $B_0 = 1.7 \times 10^5, 5.4 \times 10^4, 1.7 \times 10^4$ G. For these nine cases, we worked out the trajectories of the flux rings starting at the bottom of the convection zone from six different latitudes: $(\pi/2) - \theta = 5°, 10°, 20°, 30°, 45°, 60°$. The resultant trajectories in the meridional plane are shown in Figure 2. The positions of the rings at equal intervals of S are indicated by dots (the values of the intervals S being shown by the side of each diagram). Note that S is expressed in dimensionless units in which 1 equals 18 days. Within our approximations, these results are independent of the area of the cross section of the flux ring. We have also found they are relatively insensitive to the parameter γ (up to $\gamma = 1.67$).

Since the Coriolis force arises only when the ring is moving, it is initially zero when the ring starts from rest. The initial motion of the ring is essentially produced by the buoyancy trying to move it in the radially outward direction. We have seen that the magnetic tension may have some importance when the ring is at the bottom of the convection zone. This can be seen by looking carefully at the trajectories starting from higher latitudes, where the tension force directed toward the rotation axis has a vectorial direction significantly different from buoyancy, and hence the trajectories begin with a slight

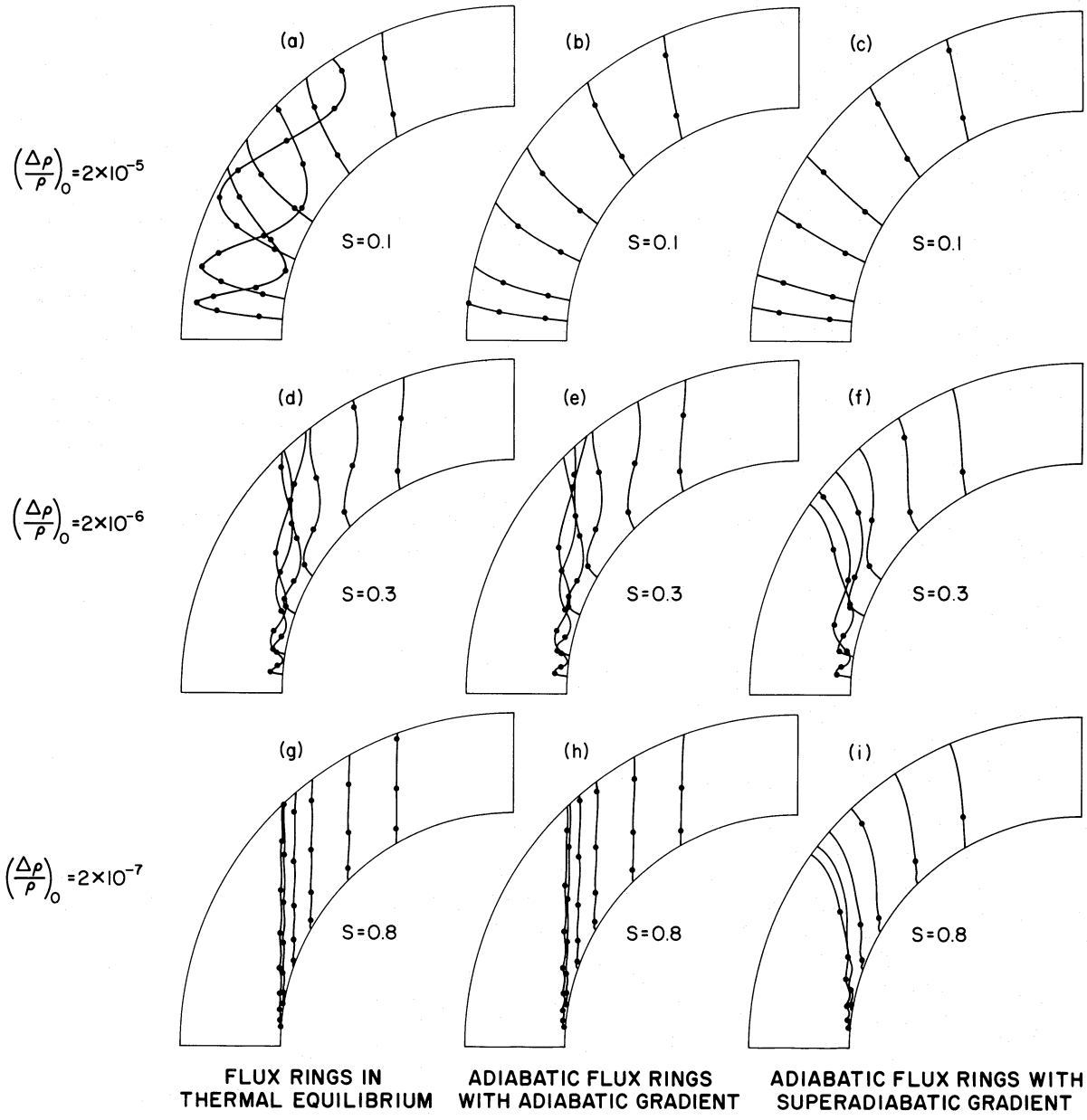

FIG. 2.—The trajectories without drag of (1) flux rings in thermal equilibrium, (2) adiabatic flux rings in adiabatic convection zone, and (3) adiabatic flux rings in superadiabatic convection zone. For each of these cases, we consider three values of $(\Delta\rho/\rho)_0 = 2 \times 10^{-5}, 2 \times 10^{-6}, 2 \times 10^{-7}$ [i.e., $M(\xi_0, \theta_0) = 10, 1, 1/10$, or equivalently $B_0 = 1.7 \times 10^5, 5.4 \times 10^4, 1.7 \times 10^4$ G]. In each of the nine cases, the flux rings start from latitudes 5°, 10°, 20°, 30°, 45°, 60°. The dots represent positions of the rings at intervals of S of which the values in dimensionless units (1 corresponds to 18 days) are shown by the side of each diagram.

departure from the radial direction [look at the 45° and 60° trajectories for the three $(\Delta\rho/\rho)_0 = 2 \times 10^{-5}$ cases]. However, besides this small effect, magnetic tension plays no important role in our problem.

The initial radial motion gives rise to a Coriolis force $-2\boldsymbol{\Omega} \times \boldsymbol{u}$ in the negative ϕ direction. This, in turn, makes the ring rotate with an azimuthal velocity u_ϕ. The component of the Coriolis force due to a negative u_ϕ is directed inward toward the rotation axis and eventually makes the trajectory turn away from the radial direction. In the following discussion, we shall be using the words "inward" and "outward" to mean inward toward and outward away from the rotation axis, respectively.

From Figure 2, we can see that, as the tube rises through the convection zone for all but the largest initial magnetic field strengths (*a*, *b*, *c*), eventually the "outward" component of buoyancy is balanced by the "inward" component of Coriolis force of the rotating ring, and the ring just moves parallel to the rotation axis due to the component of buoyancy in that direction—reminding one of the well-known Taylor-Proudman theorem (Greenspan 1968). We can easily make an order-of-magnitude estimate of this turning time. The radial velocity at time τ is of order $M(\xi, \theta)\tau$ producing a Coriolis force $2\omega M(\xi, \theta)\tau$. Hence the azimuthal velocity generated is $\omega M(\xi, \theta)\tau^2$, and the corresponding "inward" Coriolis force component is $2\omega^2 M(\xi, \theta)\tau^2$. This component compares with buoyancy $\sim M(\xi, \theta)$ at a time

$$\tau \approx \frac{1}{2^{1/2}\omega} \approx 0.16 . \tag{20}$$

We see in Figure 2 that most trajectories turn away at times of this order.

We also see that some oscillations can take place before the forces come into balance (particularly in Figs. 2*a*, 2*d*, 2*e*, and 2*f*). We show in Appendix A that these oscillations can be treated analytically with some approximations, giving a frequency of 2Ω. This is equivalent to a period of 0.71 in our dimensionless units (= 13 days) and agrees well with the numerical results. We also see that, if we do not take account of the superadiabatic gradient, the trajectories remain parallel to the axis once they turn parallel near the inner boundary (Figs. 2*d*, 2*e*, 2*g*, and 2*h*) whether flux ring is in thermal equilibrium or is adiabatic. When the superadiabatic gradient is taken into account, magnetic buoyancy becomes so strong near the top that the trajectories again tend to become radial there (Figs. 2*f* and 2*i*).

Since the flux rings eventually tend to move parallel to the axis, it is convenient to look at the components of velocity and force in cylindrical coordinates rather than spherical. Accordingly, Figure 3 shows the time evolution of the cylindrical velocity components (the axial component $\dot{\xi}\cos\theta - \xi\dot{\theta}\sin\theta$ parallel to the rotation axis, the "outward" radial component $\dot{\xi}\sin\theta + \xi\dot{\theta}\cos\theta$, and the azimuthal component $\xi\dot{\phi}\sin\theta$) for a trajectory starting at 5° latitude for all the nine cases shown in Figure 2. We see that, after the trajectories turn around, the axial velocity tends to grow due to the axial component of magnetic buoyancy whereas the "outward" radial velocity shows oscillations (particularly Figs. 3*d*–3*i*) with periods roughly agreeing with the analytical value 0.71. Apart from the situations when a rapid increase takes place due to superadiabatic gradient (Figs. 3*c*, 3*f*, and 3*i*), the "outward" radial component oscillates around zero, implying that the rings move axially in the mean. It is to be noted that we see the presence of oscillations in Figure 3 for some cases where oscillations are almost invisible in Figure 2. We can understand the reason if we look at the velocity amplitudes. For the $(\Delta\rho/\rho)_0 = 2 \times 10^{-7}$ cases, we see from Figure 3 that the oscillatory "outward" velocity has an amplitude of about 0.02 so that in a half-period it may produce an "outward" displacement of $\sim$0.007 (only about 1/40 of the depth of the convection zone). On the other hand, for the $(\Delta\rho/\rho)_0 = 2 \times 10^{-5}$ cases, the "outward" radial velocity is initially about 10 times larger, giving rise to more visible "outward" displacement amplitudes. The azimuthal component of velocity also shows oscillations, but, in contrast to the "outward" radial component, its mean value within the convection zone tends to be negative rather than zero, in order to produce an "inward" Coriolis force counteracting the "outward" component of buoyancy.

We see this "outward" force balance more clearly in Figure 4, where the time evolution of the "outward" components of buoyancy and Coriolis force, along with their resultant, for all the cases depicted in Figure 3 are shown. The "outward" buoyancy component for the flux rings in thermal equilibrium drops off with time (Figs. 4*a*, 4*d*, and 4*g*), becoming very small near the upper boundary. For an adiabatic ring in the adiabatic convection zone also, the magnetic buoyancy decreases—though less rapidly (Figs. 4*b*, 4*e*, and 4*h*). With the superadiabatic gradient taken into account, the magnetic buoyancy becomes enormous at the upper surface as expected (Figs. 4*c*, 4*f*, and 4*i*). The Coriolis force component $2\omega\xi\dot{\phi}\sin\theta$ has the expected oscillatory behavior, with its mean tending to fall to a negative value equal in magnitude to the "outward" buoyancy. Hence, the resultant "outward" force after the turning around of the trajectories is in the form of oscillations around zero, explaining why there are no net "outward" motions of the trajectories.

IV. INCLUSION OF DRAG

We now study the effect of drag on our problem. Following Parker (1979) we use the standard expression of aerodynamic drag from hydrodynamics, hoping that this will provide at least an approximate model of the drag experienced by flux tubes in the solar convection zone.

It is well known that when a cylinder moves through a fluid, the transverse drag in the high Reynolds number limit is

$$\boldsymbol{D}_\perp = -\tfrac{1}{2}C_D \rho\sigma u_\perp^2 \hat{\boldsymbol{e}}_\perp ,$$

where $u_\perp^2$ is the transverse velocity and $\hat{\boldsymbol{e}}_\perp$ is the unit vector in its direction (Goldstein 1938; Schlichting 1979). The dimensionless coefficient C_D is roughly a constant (with a value of about 0.4) for a large range of values of the Reynolds number. If we express the velocity in the dimensionless units we have been using, then the appropriate expression of drag applicable to equations (7)–(9) is

$$\boldsymbol{D}_\perp' = -\frac{C_D R_\odot}{4\pi\sigma(\xi, \theta)} u_\perp'^2 \hat{\boldsymbol{e}}_\perp , \tag{21}$$

where $u_\perp'^2 = \dot{\xi}^2 + \xi^2\dot{\theta}^2$ is the velocity square in our dimensionless coordinates. We write the drag term in the form

$$\boldsymbol{D}_\perp' = -\frac{M(\xi_0, \theta_0)}{A^{1/2}(\xi, \theta)} \left(\frac{u_\perp'}{u_t'}\right)^2 \hat{\boldsymbol{e}}_\perp . \tag{22}$$

Then if the flux ring were to reach a terminal transverse velocity at the bottom of the convection zone under the influence of

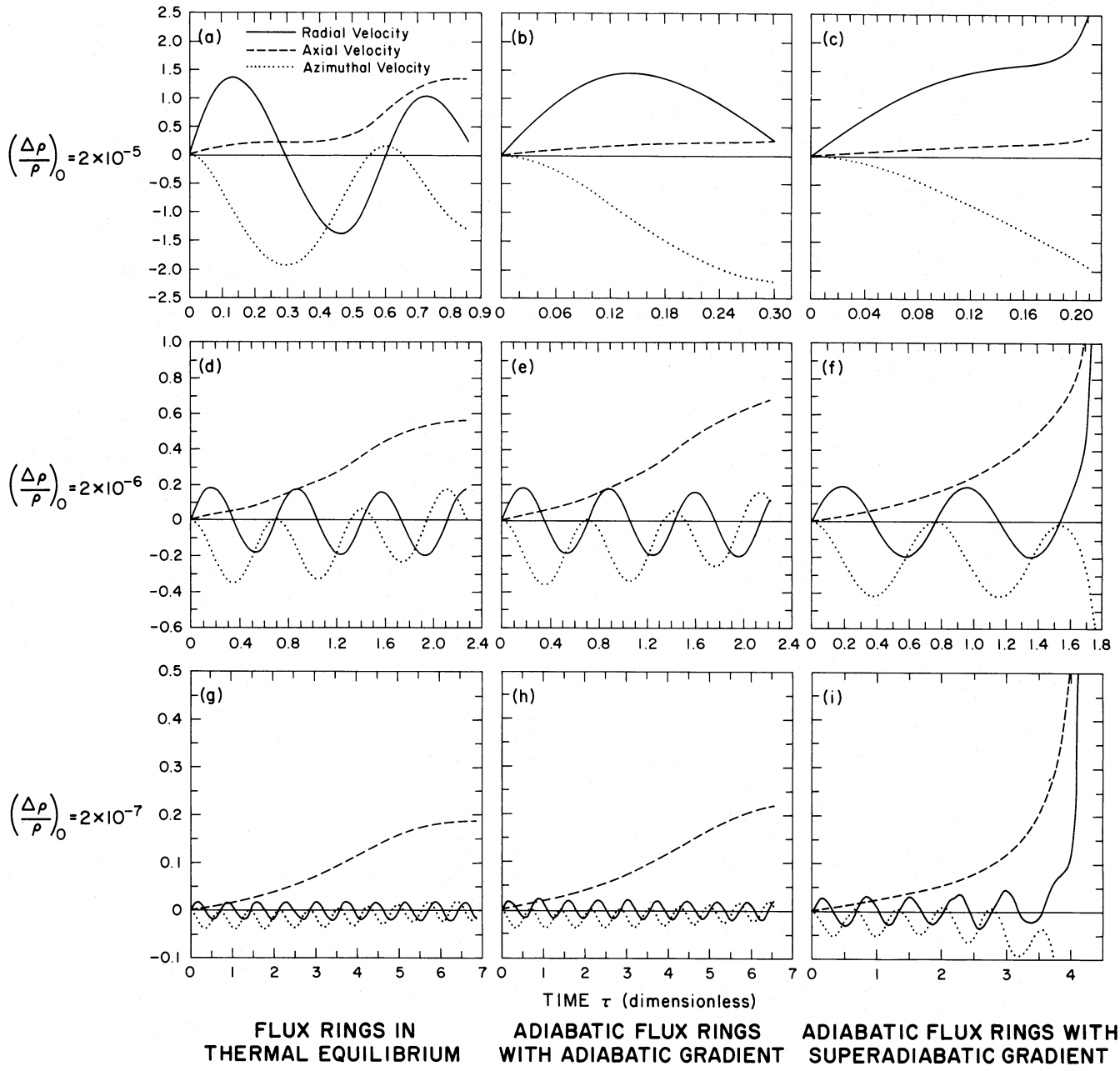

FIG. 3.—The time evolution of the cylindrical velocity components for flux rings starting from 5° latitude in each of the nine cases shown in Fig. 2. Both the time and the velocities are in dimensionless units defined in the text, the units of time and velocity being 18 days and 0.43 km s^{-1}, respectively.

buoyancy and drag alone, then the value of that terminal transverse velocity would be about u_t'. From equations (21) and (22), we can relate the radius of a flux ring cross section, $\sigma(\xi_0, \theta_0)$ with u_t' as follows:

$$\sigma(\xi_0, \theta_0) = \frac{C_D R_\odot u_t'^2}{4\pi M(\xi_0, \theta_0)} . \quad (23)$$

Table 1 shows what values of initial radius correspond to given values of u_t' and $M(\xi_0, \theta_0)$. We see that some of the entries in Table 1 are truly enormous, not satisfying the $\sigma \ll R_\odot$ condition (without drag, our results are independent of tube radius).

TABLE 1

RADIUS OF FLUX TUBE (in km) AT BOTTOM OF CONVECTION ZONE CORRESPONDING TO DIFFERENT $(\Delta\rho/\rho)_0$ AND u_t' GIVEN BY EQUATION (21)

$\left(\frac{\Delta\rho}{\rho}\right)_0$	u_t' = 1 (i.e., 0.43 km s^{-1})	u_t' = 1/3 (i.e., 0.14 km s^{-1})	u_t' = 1/9 (i.e., 0.048 km s^{-1})
2×10^{-5}....	2.2×10^3	2.5×10^2	2.7×10^1
2×10^{-6}....	2.2×10^4	2.5×10^3	2.7×10^2
2×10^{-7}....	2.2×10^5	2.5×10^4	2.7×10^3

NOTE.—$C_D = 0.4$.

However, in order to understand the behavior of our system, we will formally integrate our equations of motion for all values of $(\Delta\rho/\rho)_0 = 2 \times 10^{-6} M(\xi_0, \theta_0)$ and u_t' included in Table 1, though some of them correspond to unrealistic values of the tube radius. It is clear from equation (23) that tubes of larger radii attain higher velocities. Such tubes, moving with higher velocities, will tend to get flattened (Parker 1975) and may eventually fragment as indicated by the numerical simulations of Schüssler (1979). It is possible that this process puts an upper limit on the radii of the flux tubes rising through the convection zone.

The main effect of drag is that it puts a limit on the velocity. Several authors (Unno and Ribes 1976; Schüssler 1977; Kuznetsov and Syrovatskii 1979; Moreno-Insertis 1983) pointed out that when the conditions are such as to make the terminal velocities smaller than convective velocities, the drag due to turbulent viscosity may be more important than aerodynamic drag. It is also conceivable that the very slowly moving flux tubes will be bodily carried and distorted by convection, breaking down the implicit assumption of our model that the convection zone is a passive region through which the flux tubes rise due to magnetic buoyancy. We are going to restrict our calculations to cases where $u_t' > 0.1$, or 43 m s^{-1}, which approximately means that terminal velocities will be greater

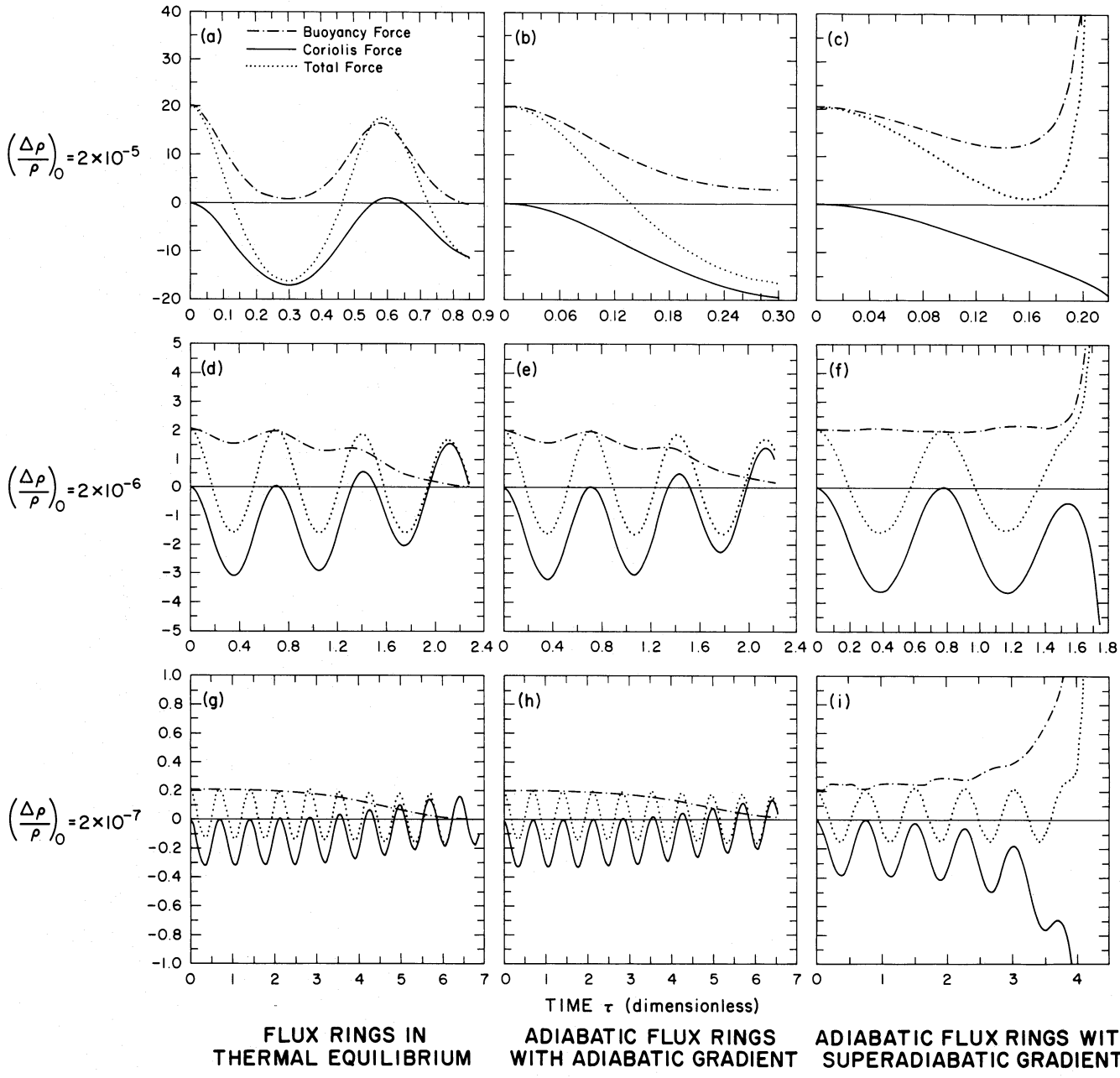

FIG. 4.—The components of force perpendicular to the rotation axis directed "outward." We show their time evolution for the same cases as depicted in Fig. 3. Again all quantities are in dimensionless coordinates.

than convective values. For longitudinal drag, we use an expression similar to equation (23):

$$D_\phi' = -\frac{M(\xi_0, \theta_0)}{A^{1/2}(\xi, \theta)} \left(\frac{\xi \dot{\phi} \sin \theta}{u_t'} \right)^2 \cdot \frac{\dot{\phi}}{|\dot{\phi}|} . \quad (24)$$

The factor $\dot{\phi}/|\dot{\phi}|$ has the value $+1$ or -1 depending on the sign of $\dot{\phi}$ and makes sure that D_ϕ' is in the opposite direction with respect to $\dot{\phi}$.

We present in Figure 5 some results showing how the trajectories for flux tubes in thermal equilibrium are modified on introducing drag. Inclusion of drag affects trajectories for adiabatic tubes in an analogous way so we do not present them here. The results for both isothermal and adiabatic flux tubes are summarized in a "regime diagram" (Fig. 6) that we discuss later. Calculations are done for the same three values of initial magnetic buoyancy factor $M(\xi_0, \theta_0) = 10, 1, 1/10$. For each of these values, we present results for three values of the drag parameter $u_t' = 1, 1/3, 1/9$ which correspond to velocities of 430, 140, 48 m s^{-1}. To get the trajectories, we again integrate the equations of motion (7)–(9) for flux tubes in thermal equilibrium, this time with the drag $\boldsymbol{D}'$ given by equations (22) and (24). The resultant trajectories are displayed in Figure 5, in which the drag increases from left to right.

In Figure 5, we see that the dots along a particular trajectory are nearly equally spaced, indicating the terminal velocity is

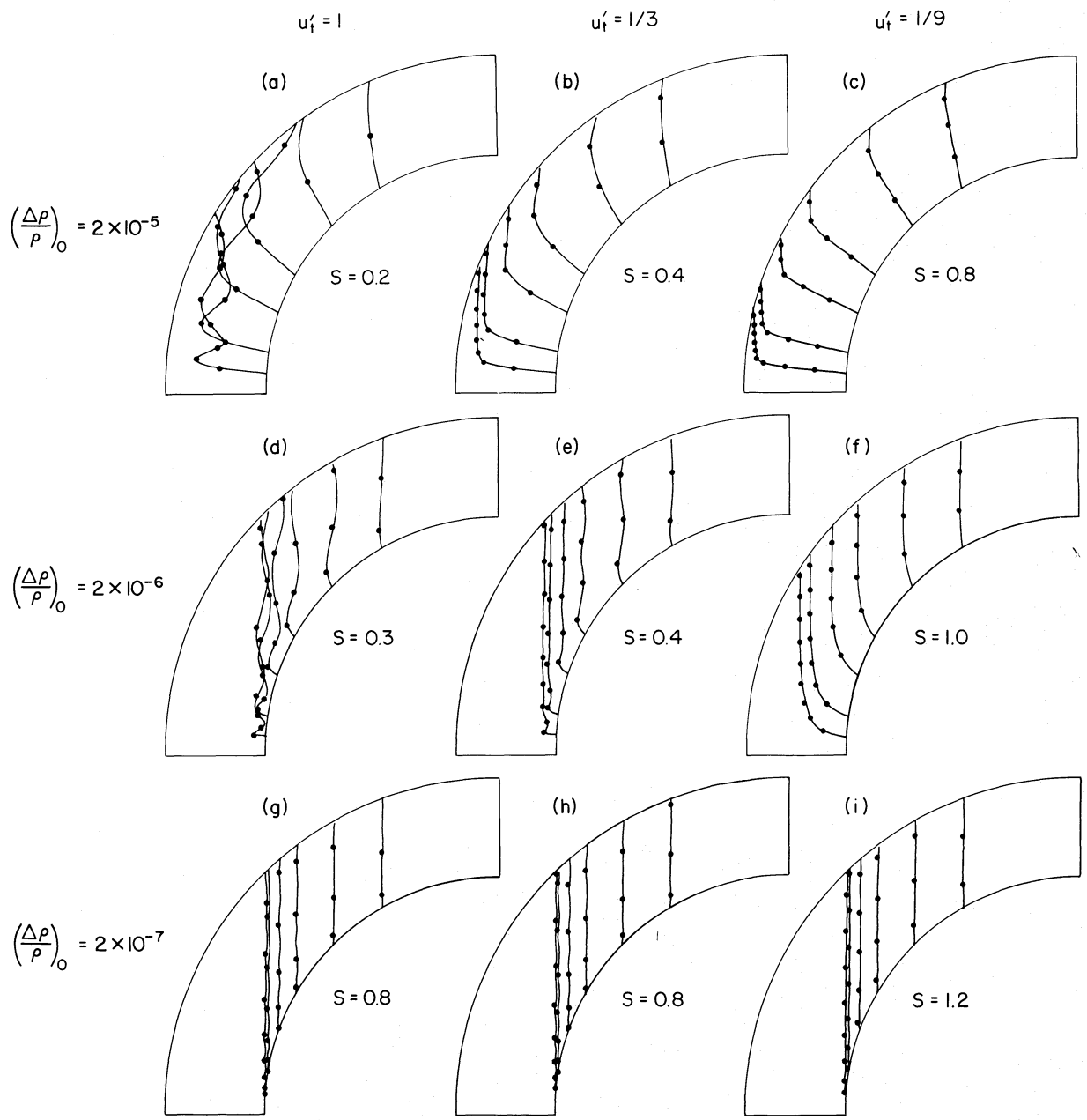

FIG. 5.—The trajectories of flux rings in thermal equilibrium incorporating drag. For each of the three values of $(\Delta\rho/\rho)_0 = 2 \times 10^{-5}, 2 \times 10^{-6}, 2 \times 10^{-7}$ [i.e., $M(\xi_0, \theta_0) = 10, 1, 1/10$, or $B_0 = 1.7 \times 10^5, 5.4 \times 10^4, 1.7 \times 10^4$ G], we consider three values of $u_t' = 1, 1/3, 1/9$ (which correspond to velocities of 430, 140, 48 m s^{-1}). For all the cases, flux rings start from latitudes 5°, 10°, 20°, 30°, 45°, 60°. The dots show positions of rings at intervals of S (1 unit = 18 days).

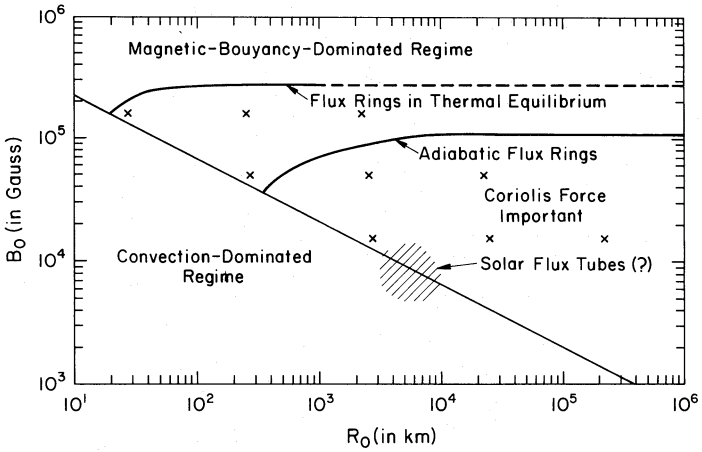

FIG. 6.—Different regimes in the parameter space of initial radius R_0 and initial magnetic field B_0 of a flux tube at the bottom of the convection zone

not a strong function of depth. It can be shown in fact that for tubes in thermal equilibrium the terminal velocity

$$u_\perp \approx T_e^{(3-2\gamma)/4(\gamma-1)}$$

in which γ is the ratio of specific heats. Thus, for γ near 1.5, $u_\perp$ is almost independent of the external temperature, and therefore depth in the convection zone. For adiabatic tubes, however, the terminal velocity increases as the tube goes up, because the buoyancy force becomes much larger in the increased superadiabatic gradient near the top of the layer.

The two most noticeable effects of drag are that larger drags slow down the flux rings and tend to dampen out the oscillations. Generally we have used larger intervals S to plot trajectories for bigger drag. The effect of drag on damping is discussed in Appendix A. We see similar effects of drag for adiabatic flux tubes also. When the drag is larger, the flux rings move radially for a longer time before turning parallel to the rotation axis. In Figure 5, in the $(\Delta\rho/\rho)_0 = 2 \times 10^{-7}$ cases (Figs. 5*g*, 5*h*, and 5*i*), the trajectories turn away before being limited by drag and the turning away time is of order 0.16 (still given by eq. [20]) so that the radial parts are virtually invisible in our plots. However, if the radial velocity is already limited by drag, which it will be for larger $\Delta\rho/\rho$, then the Coriolis force grows much less rapidly. In the presence of drag, the growing velocity of the flux ring in the meridional plane eventually gets limited in time of order $u_t'/M(\xi, \theta)$, which is small for the $M(\xi_0, \theta_0) = 10$ cases. In the extreme case of flux rings reaching the terminal speed $\sim u_t'$ almost instantaneously after start, the Coriolis force in the negative ϕ-direction is $2\omega u_t'$, producing, in time τ, an azimuthal velocity $2\omega u_t'\tau$ and a corresponding "inward" Coriolis component $(2\omega)^2 u_t'\tau$. Hence the turning time of the trajectory in this case, instead of 0.16 from equation (20), is

$$\tau \approx \frac{M(\xi, \theta)}{(2\omega)^2 u_t'} . \tag{25}$$

For $M(\xi, \theta) = 10$, we have

$$\tau \approx 0.13/u_t' ,$$

which agrees well with the top three diagrams in Figure 5 (*a*, *b*, and *c*). Equation (25) shows that the trajectories tend to move radially for a longer time when either $(\Delta\rho/\rho)_0$ or the drag force is larger (i.e., u_t' is smaller).

After turning away from the radial direction, the trajectories show damped oscillations, moving parallel to the rotation axis in the mean. As we have discussed in § III, this implies that there is some force balance preventing the ring from moving radially inward or outward in the mean. From the following simple considerations, we can have an understanding of this force balance. If α is the small angle between the mean trajectory and the direction of the rotation axis, then the Coriolis force in the negative ϕ-direction is of order $2\omega u_t' \sin\alpha$, and it reaches a force balance with drag given by equation (24) when

$$2\omega u_t' \sin\alpha \approx \frac{M(\xi_0, \theta_0)}{A^{1/2}(\xi, \theta)} \left(\frac{\xi\dot{\phi} \sin\theta}{u_t'} \right)^2 . \tag{26}$$

If the terminal azimuthal velocity obtained from equation (26) gives rise to the "inward" Coriolis force for balancing buoyancy, then

$$2\omega\xi\dot{\phi} \sin\theta \approx \frac{M(\xi, \theta)}{\xi^2} \sin\theta . \tag{27}$$

From equations (26) and (27), we find

$$\sin\alpha \approx \frac{M(\xi_0, \theta_0) M^2(\xi, \theta) \sin\theta}{(2\omega)^3 \xi^2 A^{1/2}(\xi, \theta) u_t'^3} . \tag{28}$$

We easily see that in the $M(\xi_0, \theta_0) = 0.1$, i.e., $(\Delta\rho/\rho)_0 = 2 \times 10^{-7}$, cases, a force balance is attained for a minuscule angle α. We can have an observable α only when $(\Delta\rho/\rho)_0$ is much larger. It is also clear from equation (28) that α has to be larger for smaller u_t'. We find evidence for this if we carefully look at the trajectories for $u_t' = \frac{1}{3}$ and $u_t' = \frac{1}{9}$ in both $(\Delta\rho/\rho)_0 = 2 \times 10^{-5}$ and $(\Delta\rho/\rho)_0 = 2 \times 10^{-6}$ cases (Figs. 5*b*, 5*c*, 5*e*, and 5*f*).

V. CONCLUSION

We can summarize our results in the form of a regime diagram. If drag is related to the radius through equations (22) and (23), then we have essentially a two-parameter problem. Suppose there is a flux ring at the bottom of the convection zone with given initial field B_0 and initial radius $R_0 = \sigma(\xi_0, \theta_0)$. Is the motion of the flux ring going to be affected by the Coriolis force? The answer to this question is provided in Figure 6 which shows the two-dimensional parameter space of B_0 and R_0. If the terminal velocity u_t' as given by equation (23) is less than 0.1 (dimensional velocity $\lesssim 43$ m s^{-1}), then the

velocities tend to be limited below convective velocities, and the flux rings may either be carried bodily by convection or may become very much distorted. The region of the parameter space where $u_t' < 0.1$ is denoted as the convection-dominated regime. On the other hand, if B_0 is sufficiently large, then magnetic buoyancy is so strong that flux rings move out radially and the effect of Coriolis force is not noticeable. This is the magnetic buoyancy–dominated regime. The boundary curve separating the magnetic buoyancy–dominated regime from the regime where the Coriolis force plays a significant role is determined for the two cases of (1) flux rings in thermal equilibrium with their surroundings and (2) adiabatic flux rings in a convection zone with a superadiabatic gradient. (For the case of tubes in thermal equilibrium, the dashed line indicate the boundary is not sharp, due to oscillations in the trajectories.) The actual boundary in reality probably lies somewhere between these boundaries. These boundaries were estimated on the basis of a large number of numerical runs. Since Figure 6 is a log-log plot, no matter what criterion we use to separate the two regimes, the positions of the boundary curves do not shift much. The nine cases shown in Figure 5 are indicated by X's in the parameter space. If flux tubes at the bottom of the convection zone have magnetic fields of the order of equipartition value and radii of the order of a fraction of the depth of the overshoot region, they would lie in the shaded region of the parameter space in Figure 6. But even if the flux tubes are isolated at the bottom of the convection zone and have significantly larger field strengths (up to 10^5 G), their rise to the top of the convection zone would be substantially altered by Coriolis forces.

We see that solar flux tubes of field strength $1–3 \times 10^4$ G lie close to the boundary between the convection-dominated regime and the regime where the Coriolis force is important. If the flux tubes were actually within the regime of strong Coriolis force and all the implicit assumptions of our model were correct, then flux tubes starting even from low latitudes would have been deflected substantially poleward of the sunspot region and we would not see any flux at the sunspot latitudes. Since we do see sunspots at low latitudes we have to address the question of why the flux rings are not deflected by Coriolis force as much as suggested by our calculations. One obvious possibility is that all the solar flux tubes lie within the convection-dominated regime and are carried up to the solar surface by convective motions. However, in order to consider alternative explanations, let us critically look at the implicit assumptions of our model. First, we considered the convection zone to have solid-body rotation. The presence of differential rotation could conceivably influence the trajectories of flux rings. We show in Appendix B that, if the convection zone had a distribution of equal angular momentum per unit mass throughout, i.e., if the rotation law was

$$\Omega(r, \theta) \alpha \frac{1}{r^2 \sin^2 \theta},$$

then the flux rings would come out radially (neglecting magnetic tension). However, the Ω = constant case we considered is probably much closer to reality for the solar convection zone (see Duvall *et al.* 1984), and the prospect of solving our problem by invoking differential rotation seems quite remote.

The second questionable assumption used in our calculations is the assumption that the flux rings remain symmetric during most of their ascent through the convection zone, as concluded by Schüssler (1980). We have shown that, under a wide range of thermal and drag conditions, such flux rings will emerge at much higher latitudes than where sunspots are found, unless their velocities of rise due to magnetic buoyancy are sufficiently small (< 50 m s^{-1}) that they are principally carried up by convection. Probably loop formation takes place within the convection zone, and the resultant nonaxisymmetry may be crucial in counteracting the Coriolis force to some extent. First of all, if the magnetic field is frozen in the flux rings and the rings are to remain symmetric, then the magnetic field strengths keep dropping as the rings move upward into regions of lower pressure. However, if loop formation takes place, then gas may flow from the higher parts of the loop to the lower parts to decrease the gravitational potential, consequently keeping the field more compressed and hence retaining more magnetic buoyancy in the upper parts of the loop. In addition, if a flux ring does not get loosened as a whole, but has parts of it anchored to the bottom of the convection zone, then we expect the tension in the ring to play an important role in stopping the upper parts of a loop from moving to significantly higher latitudes. We plan to study the effects of nonaxisymmetry in a subsequent paper. Since carrying out the calculations presented above, we have discovered that Moreno-Insertis (1986) has developed a numerical model for nonaxisymmetric loops rising in the convection zone for Cartesian geometry and without rotation that confirm many of these thoughts.

It is interesting to consider the implications of our calculations for other stars with convective envelopes. The dimensionless equations (7)–(9) can at once be used to make calculations for other stars, using an appropriate value of the rotation parameter ω and integrating from an appropriate depth ξ_0. If nonaxisymmetry and partial anchoring at the bottom are responsible for counteracting the Coriolis force in the Sun, then probably they will be similarly operative in other stars also, causing the flux to appear at low latitudes. On the other hand, if the reason solar magnetic fields appear at low latitudes is that the flux tubes lie in the convection-dominated regime, then presumably there will be stars in which flux tubes would lie in the regime of strong Coriolis force and would appear on the stellar surface near the poles. Thus, a study of magnetic stars may eventually throw more light on the magnetic buoyancy problem in the solar context. At present, on the basis of the calculations we have done so far, it seems clear that Coriolis forces should be taken into consideration when studying motions of flux tubes through stellar convection zones.

We are grateful to Jack Miller for his help and advice in developing the code, and to Tom Bogdan for his constructive criticism of an initial draft of the manuscript and for suggesting improvements. We also thank Gene Parker and Ed DeLuca for helpful comments.

APPENDIX A

THE OSCILLATIONS OF FLUX RING TRAJECTORIES

In order to have some insight into the nature of the oscillations of our flux ring trajectories, we consider a point on the flux ring and construct a local Cartesian coordinate system there. We take the z-axis in the direction of the rotation axis, the x-axis in the radially outward direction from the rotation axis, and the y-axis in the azimuthal direction (i.e., the ϕ-direction). Let us start from equation (3) neglecting the magnetic tension term. It is possible to obtain an analytical solution if we make the following assumptions:

1. The drag $\boldsymbol{D}$ increases linearly with velocity, i.e., $\boldsymbol{D} = -k\boldsymbol{u}$.
2. The WKB approximation, which neglects variations of m_i, m_e, and of the components g_x, g_z of gravity over a wavelength of oscillation, is justified.

It is true that we considered the drag to depend quadratically on velocity in our numerical calculation, and the WKB approximation is presumably not a good approximation for the adiabatic convection zone we used. However, in spite of these caveats, we shall see that the analytical results obtained with these assumptions qualitatively reproduce the broad features of the oscillations arising in the numerical calculations, providing some insight into their origin.

The three components of equation (3) will be

$$\left(\frac{d}{dt} + k\right)u_x - 2\Omega u_y = Mg_x\,, \tag{A1}$$

$$\left(\frac{d}{dt} + k\right)u_y + 2\Omega u_x = 0\,, \tag{A2}$$

and

$$\left(\frac{d}{dt} + k\right)u_z = Mg_z\,, \tag{A3}$$

where $M = (m_i - m_e)/2m_i$. We thus see that the motions in the x- and y-directions are coupled together, but the z-motion is not coupled to them. Integration of equation (A3) gives

$$u_z = \frac{Mg_z}{k}\left[1 - \left(1 - \frac{ku_z(o)}{Mg_z}\right)e^{-kt}\right], \tag{A4}$$

i.e., u_z tends to approach the asymptotic value Mg_z/k. Combining equations (A1) and (A2), we find

$$\left(\frac{d}{dt} + k\right)^2 u_x + 4\Omega^2 u_x = kMg_x$$

of which the solution is

$$u_x = e^{-kt}(c_1 e^{i2\Omega t} + c_2 e^{-i2\Omega t}) + \frac{kMg_x}{4\Omega^2 + k^2}\,. \tag{A5}$$

We thus obtain damped oscillations with frequency 2Ω. This result reminds one of the well-known inertial oscillations in rotating fluids with a maximum allowed frequency of 2Ω (see, for example, Greenspan 1968). The frequency of 2Ω corresponds to a period of 0.71 in our units, whereas our numerical calculations give periods between 0.6 and 0.8. We also see that the damping is quicker for larger k, implying that there should be more damping for trajectories with lower terminal velocities. This also agrees with numerical results. Thus we see that the above simple-minded analysis reproduces the broad qualitative features of the oscillations observed in the numerical simulations.

APPENDIX B

THE EFFECT OF DIFFERENTIAL ROTATION

In order to consider motions of flux rings in a differentially rotating convection zone, one should write down the equations of motion in an inertial frame and then write

$$\frac{d\phi}{dt} = \Omega(r, \theta) + \left(\frac{d\phi}{dt}\right)_{\rm rel}\,, \tag{B1}$$

where $\Omega(r, \theta)$ is the angular velocity of the convection zone and $(d\phi/dt)_{\rm rel}$ is that of the flux ring relative to the convection zone. We can get the desired equations of motion by putting $\Omega = 0$ in equations (4)–(6) and then substituting for $d\phi/dt$ from equation (B1),

remembering that we need not keep terms involving $\Omega^2(r, \theta)$, which represent the centrifugal force present even in the absence of a moving flux ring and which we have been neglecting compared to gravity. This procedure gives

$$2m_i\left[\frac{d^2r}{dt^2} - r\left(\frac{d\theta}{dt}\right)^2 - r\left(\frac{d\phi}{dt}\right)^2_{\rm rel}\sin^2\theta - 2r\Omega(r,\theta)\left(\frac{d\phi}{dt}\right)_{\rm rel}\sin^2\theta\right] = -(m_i - m_e)g_s\left(\frac{R_\odot}{r}\right)^2 - \frac{\Psi^2}{2\pi\sigma^2}\sin\theta + D_r\,, \tag{B2}$$

$$2m_i\left[r\frac{d^2\theta}{dt^2} + 2\frac{dr}{dt}\frac{d\theta}{dt} - r\left(\frac{d\phi}{dt}\right)^2_{\rm rel}\sin\theta\cos\theta - 2r\Omega(r,\theta)\left(\frac{d\phi}{dt}\right)_{\rm rel}\sin\theta\cos\theta\right] = -\frac{\Psi^2}{2\pi\sigma^2}\cos\theta + D_\theta\,, \tag{B3}$$

$$\frac{2m_i}{r\sin\theta}\frac{d}{dt}\left[r^2\left(\Omega(r,\theta) + \left(\frac{d\phi}{dt}\right)_{\rm rel}\right)\sin^2\theta\right] = D_\phi\,. \tag{B4}$$

It is now straightforward to show that for an angular velocity distribution

$$\Omega(r,\theta)\alpha\,\frac{1}{r^2\sin^2\theta}\,, \tag{B5}$$

a flux ring would move radially when we neglect tension. Noting that the azimuthal drag D_ϕ must be zero when $(d\phi/dt)_{\rm rel} = 0$, we at once see that

$$\left(\frac{d\phi}{dt}\right)_{\rm rel} = 0 \tag{B6}$$

is a solution of equation (B4) if $\Omega(r, \theta)$ is given by equation (B5). Neglect of the tension term $\Psi^3\cos\theta/2\pi\sigma^2$ in equation (B3) now imples that

$$\frac{d\theta}{dt} = 0 \tag{B7}$$

is a solution of that equation when equation (B6) holds. Hence, the flux ring moves in the radial direction, with its motion described by equation (B2) considerably simplified on account of equations (B6) and (B7). The reason this happens is that the flux tube conserves angular momentum when moving (neglecting tension) and is moving in a medium whose angular momentum is independent of radius, so there is no restoring perturbation centrifugal force.

REFERENCES

Acheson, D. J. 1978, *Phil. Trans. Roy. Soc.*, **A289**, 459.
———. 1979, *Solar Phys.*, **62**, 23.
Acheson, D. J., and Gibbons, M. P. 1978, *Solar Phys.*, **85**, 743.
Acheson, D. J., and Hide, R. 1973, *Rep. Prog. Phys.*, **36**, 159.
Choudhuri, A. R. 1984, *Ap. J.*, **281**, 846.
Däppen, W., and Gough, D. O. 1984, in *Theoretical Problems in Stellar Stability and Oscillations*, ed. M. Gabriel and A. Noels (Liège: Institute d'Astrophysique), p. 264.
DeLuca, E. E., and Gilman, P. A. 1986, *Geophys. Ap. Fluid Dyn.*, **37**, 85.
Duvall, J. L., Jr., Dziembowski, W. A., Goode, P. R., Gough, D. O., Harvey, J. W., and Leibacher, J. W. 1984, *Nature*, **310**, 22.
Galloway, D. J., and Weiss, N. O. 1981, *Ap. J.*, **243**, 945.
Gilman, P. A. 1970, *Ap. J.*, **162**, 1019.
———. 1983, *Ap. J. Suppl.*, **53**, 243.
Gilman, P. A., and Miller, J. 1981, *Ap. J. Supp.*, **46**, 211.
Glatzmaier, G. A. 1985, *Ap. J.*, **291**, 300.
Goldstein, S. 1938, *Modern Developments in Fluid Mechanics* (Oxford: Clarendon Press), p. 418–419.
Greenspan, H. P. 1968, *The Theory of Rotating Fluids* (Cambridge: Cambridge University Press).
Hughes, D. W. 1985, *Geophys. Ap. Fluid Dyn.*, **34**, 99.
Kuznetsov, V. D., and Syrovatskii, S. J. 1979, *Soviet Astr.–AJ*, **23**, 715.
Lamb, H. 1945, *Hydrodynamics* (New York: Dover).
Moffatt, H. K. 1978, *Magnetic Field Generation in Electrically Conducting Fluids* (Cambridge: Cambridge University Press).
Moreno-Insertis, F. 1983, *Astr. Ap.*, **122**, 241.
———. 1986, *Astr. Ap.*, **166**, 291.
Parker, E. N. 1955, *Ap. J.*, **121**, 491.
———. 1975, *Ap. J.*, **198**, 205.
———. 1979, *Cosmical Magnetic Fields* (Oxford: Clarendon Press).
———. 1984, *Ap. J.*, **281**, 839.
———. 1986, preprint.
Roberts, P. H., and Stewartson, K. 1977, *Astr. Nach.*, **298**, 311.
Schlichting, H. 1979, *Boundary-Layer Theory* (7th ed., New York: McGraw-Hill), p. 15–19.
Schmitt, J. H. M. M., and Rosner, R. 1983, *Ap. J.*, **265**, 901.
Schmitt, J. H. M. M., Rosner, R., and Bohn, H. U. 1984, *Ap. J.*, **282**, 316.
Schüssler, M. 1977, *Astr. Ap.*, **56**, 439.
———. 1979, *Astr. Ap.*, **71**, 79.
———. 1980, *Astr. Ap.*, **89**, 26.
Spiegel, E. A., and Weiss, N. O. 1980, *Nature*, **287**, 616.
Spruit, H. C. 1974, *Solar Phys.*, **34**, 277.
Spruit, H. C., and van Ballegooijen, A. A. 1982, *Astr. Ap.*, **106**, 58.
Symon, K. R. 1971, *Mechanics* (Reading, Mass: Addison-Wesley).
Unno, W., and Ribes, E. 1976, *Ap. J.*, **208**, 222.
van Ballegooijen, A. A. 1982, *Astr. Ap.*, **113**, 99.
———. 1983, *Astr. Ap.*, **118**, 275.

ARNAB RAI CHOUDHURI and PETER A. GILMAN: High Altitude Observatory, National Center for Atmospheric Research, P.O. Box 3000, Boulder, CO 80307